ACS Chemical Neuroscience

Research Article

pubs.acs.org/chemneuro

Development of [^{11}C]MFTC for PET Imaging of Fatty Acid Amide Hydrolase in Rat and Monkey Brains

Katsushi Kumata,[†] Joji Yui,[†] Akiko Hatori,[†] Jun Maeda,[†] Lin Xie,[†] Masanao Ogawa,[†,‡] Tomoteru Yamasaki,[†] Yuji Nagai,[†] Yoko Shimoda,[†] Masayuki Fujinaga,[†] Kazunori Kawamura,[†] and Ming-Rong Zhang*[,†]

[†]Molecular Imaging Center, National Institute of Radiological Sciences, Chiba 263-8555, Japan

[‡]SHI Accelerator Service Co. Ltd., Tokyo 141-8686, Japan

Supporting Information

ABSTRACT: We developed 2-methylpyridin-3-yl-4-(5-(2-fluorophenyl)-4*H*-1,2,4-triazol-3-yl)piperidine-1-[^{11}C]carboxylate ([^{11}C]MFTC) as a promising PET tracer for in vivo imaging of fatty acid amide hydrolase (FAAH) in rat and monkey brains. [^{11}C]MFTC was synthesized by reacting 3-hydroxy-2-methylpyridine (**2**) with [^{11}C]phosgene ([^{11}C]$COCl_2$), followed by reacting with 4-(5-(2-fluorophenyl)-4*H*-1,2,4-triazol-3-yl)piperidine (**3**), with a 20 ± 4.6% radiochemical yield (decay-corrected, n = 30) based on [^{11}C]CO_2 and 40 min synthesis time from the end of bombardment. A biodistribution study in mice showed high uptake of radioactivity in FAAH-rich organs, including the lung, liver, and kidneys. Positron emission tomography (PET) summation images of rat brains showed high radioactivity in the frontal cortex, cerebellum, and hippocampus, which was consistent with the regional distribution pattern of FAAH in rodent brain. Pretreatment with MFTC or FAAH-selective URB597 significantly reduced the uptake in the brain. PET imaging of monkey brain showed relatively high uptake in the whole brain, particularly in the occipital cortex, which was also inhibited by treatment with MFTC or URB597. More than 96% of the total radioactivity was irreversible in the brain homogenate of rats 5 min after the radiotracer injection. The specific in vivo FAAH binding indicates that [^{11}C]MFTC is a promising PET tracer for visualizing FAAH in the brain.

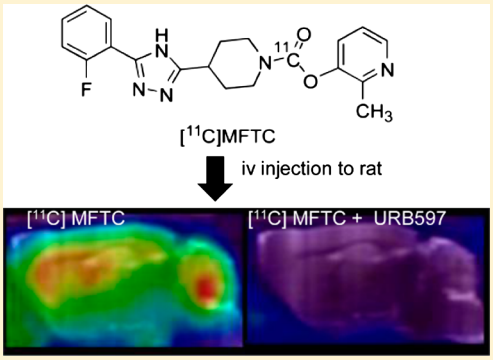

KEYWORDS: *PET, fatty acid amide hydrolase, FAAH, [^{11}C]MFTC, [^{11}C]$COCl_2$, irreversible specific binding*

The lipid character of endocannabinoids, such as anandamide and 2-arachidonoyl glycerol, indicates that these signaling molecules that target cannabinoid receptors cannot be stored in vesicles, unlike polar G-protein coupled receptor neurotransmitters.[1] Endocannabinoids are synthesized upon request and are rapidly and efficiently degraded to maintain their endogenous levels. In the central nervous system, anandamide levels are primarily regulated by fatty acid amide hydrolase (FAAH), a hydrolyzing enzyme that converts anandamide into arachidonic acids and ethanolamine.[2,3] As determined in the post-mortem human brains, FAAH is widely distributed within the gray matter of the cerebral cortex, cerebellum, basal ganglia, and thalamus.[4] It has been reported that selective inhibitors for FAAH showed evident pharmacological effects on pain, anxiety, addiction, and psychiatric disorders.[5]

Because FAAH plays an important role in a variety of disorders, there is increased interest in developing radiotracers for positron emission tomography (PET) imaging of FAAH in the brain. To our knowledge, there are only two PET tracers for FAAH used in clinical studies of the human brain. The first is [^{11}C]CURB (Figure 1), an irreversible inhibitor of FAAH that is an analogue of the FAAH-selective ligand URB597.[6] This radiotracer contains a ^{11}C-labeled carbamate moiety that expresses FAAH activity and has been used to characterize FAAH in the human brain.[7] Motivated by the success of [^{11}C]CURB, several research groups have been pursing alternate PET tracers and exploring relationships among chemical structure, in vitro binding affinity, and in vivo specificity for FAAH.[8−13] Most of the promising PET tracers contain an [^{11}C-carbonyl]carbamate or urea unit and are irreversible FAAH inhibitors according to rationale of measuring FAAH in vivo (Figure 1). In addition to the irreversible tracers, [^{11}C]MK-3168 is a reversible inhibitor that is currently being studied in human subjects, although no clinical results have been reported.[14,15]

Considering that a gold standard for PET imaging of FAAH has not emerged yet, in this study, we aimed to develop a novel PET tracer containing an [^{11}C-carbonyl]carbamate moiety for in vivo imaging of FAAH in rat and monkey brains, with the expectation that this tracer could also be used for visualization and characterization FAAH in human brain. Our present

Received: October 24, 2014
Revised: November 13, 2014
Published: November 14, 2014

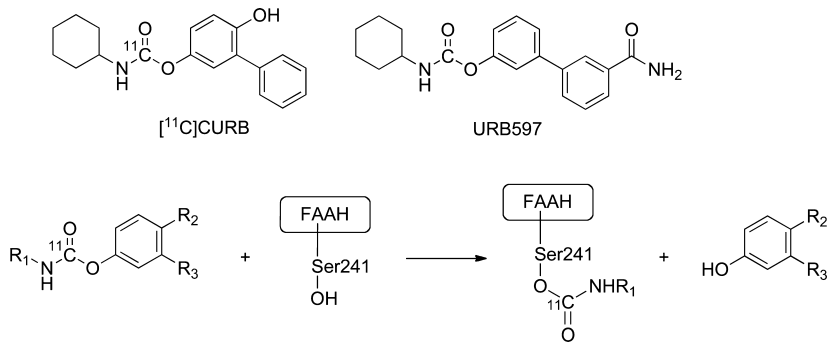

Figure 1. Chemical structures of [11C]CURB and URB597 and mechanism of [11C]carbonate labeling of FAAH.

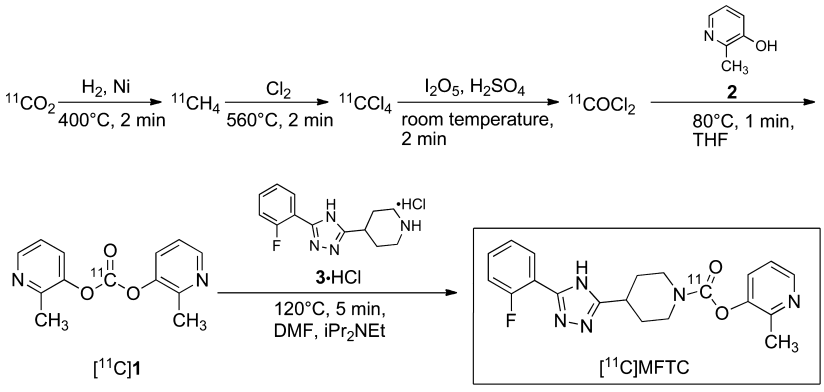

Figure 2. Production of $[^{11}C]COCl_2$ and radiosynthesis of [11C]MFTC via bispyridyl-[11C]carbonate ([11C]**1**).

targeted compound was 2-methylpyridin-3-yl-4-(5-(2-fluorophenyl)-4*H*-1,2,4-triazol-3-yl)piperidine-1-carboxylate (MFTC, Figure 2), which is reported to have a high binding affinity (IC_{50} = 0.34 nM) for FAAH in a patent application.[16] Because of the carbamate structure, MFTC, like CURB and URB597, is thought to be an irreversible inhibitor for FAAH.

In this study, we synthesized [11C]MFTC using [11C]-phosgene ($[^{11}C]COCl_2$) as a labeling agent via bis(2-methylpyridin-3-yl)-[11C]carbonate ([11C]**1**, Figure 2) as a novel radioactive intermediate. We evaluated the potential of [11C]MFTC for in vivo imaging of FAAH in rat and monkey brains by determining in vitro binding affinity and biodistribution, and performing PET scans.

RESULTS AND DISCUSSION

Our selection of MFTC for labeling with ^{11}C (β+ emitter, $t_{1/2}$ = 20.4 min) and evaluation as a possible PET tracer for brain FAAH was initially guided by its high affinity toward FAAH and its computed lipophilicity (clogD value: 3.6), which is consistent with achieving adequate brain entry.[17] In this regard, MFTC (IC_{50} = 0.34 nM) presented superior in vitro binding affinity for FAAH with respect to URB597 (IC_{50} = 0.58 nM).[16]

Radiochemistry. The radiosynthesis of [11C]MFTC was performed from the production of $[^{11}C]COCl_2$ to the formulation of the product using a totally automated system developed in house.[18,19]

Previous studies indicated that the [11C]carbamate moiety in [11C]CURB was necessary for binding FAAH in vivo according to the mechanism of [11C]CURB radiolabeling of FAAH (Figure 1).[6] In the present study, we labeled the carbamate moiety in MFTC using $[^{11}C]COCl_2$ (Figure 2). So far, [11C]CO, $[^{11}C]CO_2$, and $[^{11}C]COCl_2$ have been used to construct a [11C]carbamate moiety. Compared to [11C]CO, $[^{11}C]CO_2$ is more convenient for labeling carbamate due to the $[^{11}C]CO_2$-fixation method.[20] We have used this method to synthesize several [11C]carbamate analogues,[21] but we were not unable to obtain [11C]MFTC with $[^{11}C]CO_2$ in reproducible radiochemical yields. The reason remains unclear.

We used $[^{11}C]COCl_2$ to achieve the automated synthesis of [11C]MFTC (Figure 2), because it is the most reactive carbonylating agent available in our facility for routine use. Reaction of $[^{11}C]COCl_2$ with 3-hydroxy-2-methylpyridine (**2**) gave bispyridyl-[11C]carbonate [11C]**1** in high yields, followed by reaction of [11C]**1** with 4-(5-(2-fluorophenyl)-4*H*-1,2,4-triazol-3-yl)piperidine (**3**) to give [11C]MFTC. Here, the carbonate compound [11C]**1** was used as a new radioactive intermediate because the phenoxycarbonylation of amines is a useful method for the synthesis of carbamate analogues. The identity of [11C]**1** was confirmed by simulating the reaction of nonradioactive $COCl_2$ with **2**. Without separation from the reaction mixture, [11C]**1** was subsequently reacted with **3** to accomplish the radiosynthesis efficiently. Thus, [11C]carbonate as a reactive intermediate could be used to construct an [11C]carbamate moiety with $[^{11}C]COCl_2$. After the two-step reaction, separation, and formulation, [11C]MFTC was obtained in 20 ± 4.6% radiochemical yield based on $[^{11}C]CO_2$ (decay-corrected), with sufficient radioactivity and reliable quality for animal evaluation. Starting from 18.7 ± 3.4 GBq of $[^{11}C]CO_2$, 2.0 ± 0.6 GBq of [11C]MFTC was obtained at the end of synthesis (n = 30). The total synthesis time averaged 40 min from the end of bombardment. The radiochemical purity of [11C]MFTC was greater than 96%, and the specific activity was 50 ± 26 GBq/μmol. No significant UV peaks relating to the two precursors or other chemical impurities were observed on the HPLC chromatogram of the final product. No radiolysis was observed up to 120 min after

dx.doi.org/10.1021/cn500269g | ACS Chem. Neurosci. 2015, 6, 339−346

formulation, indicating radiochemical stability within the duration of at least one PET scan. The analytical results were in compliance with the quality control/assurance specifications of radiopharmaceuticals produced in our facility.

In Vitro Binding Assays. We used competitive activity-based protein profiling[8] to assess the potency of MFTC and URB597 for FAAH. Figure 3 shows the binding curves of

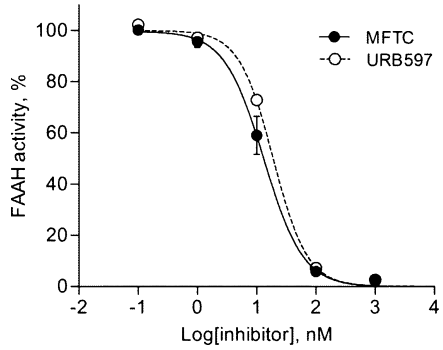

Figure 3. In vitro binding assay for FAAH.

MFTC and URB597 as a control for FAAH in rat brain. From these curves, the in vitro binding affinities (IC_{50}s) of MFTC and URB597 for FAAH were calculated to be 13.6 ± 2 and 18.3 ± 2 nM, respectively. Moreover, MFTC and URB597 showed a concentration-dependent inhibitory effect only for the FAAH band on the gel images (Supporting Information Figure 1). Although MFTC was not directly compared to CURB, we assumed that MFTC may show at least a similar binding affinity for FAAH as CURB because URB597 was previously reported to be more potent than CURB.[6] Thus, the binding affinity of MFTC might be sufficient for PET imaging of brain FAAH in vivo.

Biodistribution Study. The distribution of radioactivity in mice was measured at different time points after injection of [^{11}C]MFTC (Table 1). At 1 min, high uptake was observed in the blood, brain, heart, lungs, kidneys, and small intestine. After the initial phase, the radioactivity levels in the blood, heart, lung, and muscle decreased rapidly. The uptake in the liver, spleen, kidney, and small intestine reached a maximum at 5 min and then decreased slowly. High initial uptake (2.69% ID/g) at 1 min was observed in the mouse brain, and the brain uptake remained at 2.78% ID/g at 60 min after the injection.

The present result indicates that the distribution of radioactivity was in agreement with the distribution of FAAH in rodents as reported previously,[22,23] with high expression in the brain, liver, testes, uterus, kidneys, spleen, and possibly lungs, but not in the muscle and heart. The kinetics of uptake for [^{11}C]MFTC suggests that the radioactivity was mainly cleared via the hepatobiliary and intestinal reuptake pathways with rapid washout from the body. The brain uptake indicated that [^{11}C]MFTC could pass the blood-brain barrier and enter the brain rapidly, which is a prerequisite for a suitable PET tracer for brain imaging. The brain uptake may be related to the lipophilicity (cLogD: 3.6) of [^{11}C]MFTC and the putative lack of interaction of this radiotracer with efflux pump on the blood-brain barrier. Within 60 min after injection, no significant decrease in uptake was observed in the brain, suggesting irreversible binding in the brain.

PET Study in Rats. Figure 4 shows representative PET images of rat brains after injection of [^{11}C]MFTC (A), [^{11}C]MFTC and MFTC (B), or [^{11}C]MFTC and URB597 (C). Control PET images showed considerable penetration and accumulation of radioactivity in the brain (Figure 4A). The highest radioactivity was seen in the cerebellar nucleus, followed by the frontal cortex, cerebellar cortex, and hippocampus, while the lowest uptake was observed in the pons. As shown in the time−activity curves (TACs) of the brain (Figure 5A), radioactivity in brain tissues increased rapidly after the injection, peaked at 10 min, and maintained this level until the end of PET scans. As shown on the PET images (Figure 4B) and TACs (Figure 5B), pretreatment with MFTC markedly reduced the brain uptake compared to the control. A significant decrease in uptake was seen in all brain regions, and the fairly low level of radioactivity was uniformly disturbed throughout the brain. The maximum reduction in uptake exceeded 80% within the all brain regions. Pretreatment with URB597 also showed a significant decrease in brain uptake, and almost abolished the difference in radioactivity among all brain regions. The radioactivity levels at 90 min after the radiotracer injection were reduced by 62−86% and the radioactivity distribution became regionally homogeneous.

The distribution pattern of radioactivity for [^{11}C]MFTC was similar to that for [^{11}C]CURB[6] and distribution of FAAH in the rat brain.[24,25] Inhibitory experiment using MFTC or URB597 significantly reduced the regional uptake, indicating high specific binding of [^{11}C]MFTC in the rat brain. Because our present in vitro binding assay demonstrated that MFTC and URB597 strongly bind FAAH in the brain, their ability to block brain uptake provides evidence that [^{11}C]MFTC binds to FAAH in the rat brain. The specific binding for FAAH in the brain regions was further confirmed by ex vivo autoradiographic images of rat brains (see Supporting Information Figure 2).

Table 1. Distribution of Radioactivity in Mice after Injection of [^{11}C]MFTC[a]

tissue	1 min	5 min	15 min	30 min	60 min
blood	3.07 ± 0.14	1.24 ± 0.09	0.75 ± 0.06	0.61 ± 0.05	0.44 ± 0.02
heart	3.04 ± 0.41	0.65 ± 0.11	0.48 ± 0.03	0.42 ± 0.09	0.34 ± 0.06
lungs	8.19 ± 0.94	6.75 ± 0.79	6.31 ± 1.36	5.45 ± 1.39	5.54 ± 0.96
liver	3.77 ± 1.10	7.79 ± 1.56	6.33 ± 0.23	5.73 ± 0.85	4.51 ± 0.59
spleen	1.56 ± 0.26	1.85 ± 0.26	1.40 ± 0.30	1.29 ± 0.45	1.15 ± 0.14
kidneys	16.67 ± 2.46	17.52 ± 1.01	15.92 ± 2.22	13.80 ± 1.10	12.60 ± 0.97
small intestine	3.58 ± 0.31	6.19 ± 0.37	4.29 ± 0.53	3.20 ± 0.31	2.51 ± 0.32
testes	0.78 ± 0.09	0.89 ± 0.07	0.83 ± 0.10	0.87 ± 0.09	0.89 ± 0.10
muscle	1.89 ± 0.36	0.38 ± 0.09	0.19 ± 0.03	0.16 ± 0.02	0.12 ± 0.02
brain	2.69 ± 0.20	2.77 ± 0.30	2.73 ± 0.24	2.68 ± 0.28	2.78 ± 0.51

[a]Data are % ID/g tissue (mean ± SD; n = 4).

dx.doi.org/10.1021/cn500269g | ACS Chem. Neurosci. 2015, 6, 339−346

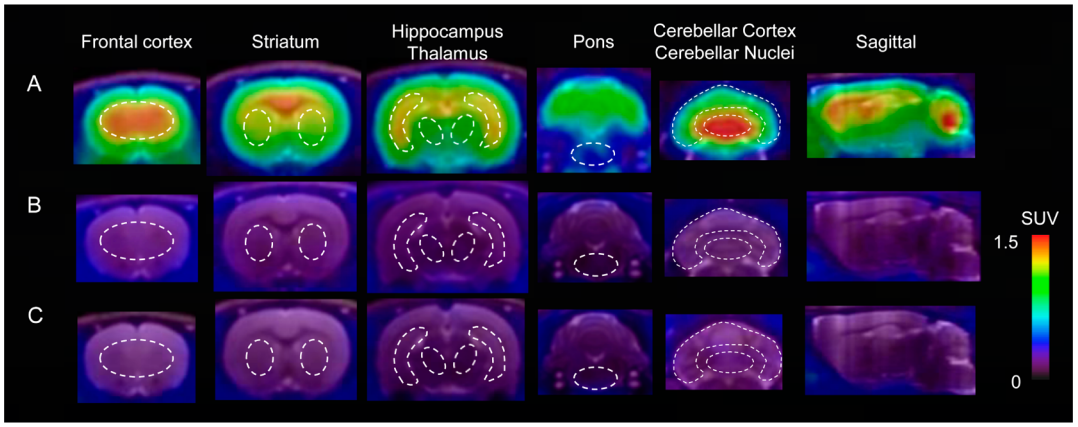

Figure 4. Representative coronal and sagittal PET/MR images for [^{11}C]MFTC in rat brains (n = 4 for each group). (A) [^{11}C]MFTC only. (B) Pretreatment with MFTC. (C) Pretreatment with URB597.

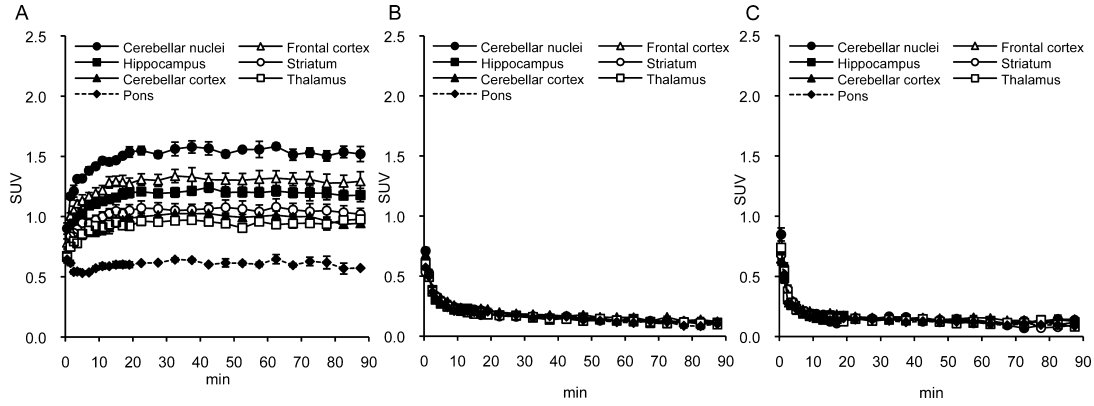

Figure 5. Time–activity curves for [^{11}C]MFTC in rat brains (n = 4 for each group). (A) [^{11}C]MFTC only. (B) Pretreatment with MFTC. (C) Pretreatment with URB597.

Measurement of the Irreversible Binding. By measuring the radioactivity in the extracts and residual pellet, the amount of binding bound to brain tissue was determined (Table 2). At

Table 2. Percentage (%) of [^{11}C]MFTC Bound to Rat Brain Tissue after Injection

time (min)	mean ± SD
1	95.55 ± 1.10
3	97.28 ± 0.36
5	98.45 ± 0.42
pretreatment with URB597	
5	2.28 ± 0.47

1 min after injection, 95% of radioactivity in the brain homogenate was found to irreversibly bind to tissue. The specificity of the irreversible binding was confirmed by performing the same procedure in rats pretreated with URB597. This treatment almost abolished the irreversible binding with only 2% radioactivity was left in the brain homogenate 5 min after the radiotracer injection. The extraction experiments in homogenized brain demonstrated that [^{11}C]MFTC was irreversibly bound to FAAH in the rat brain.

PET Study in Monkey. Figures 6 and 7 show PET images and TACs of [^{11}C]MFTC in the monkey brain. Control summation images between 5 and 90 min after radiotracer injection showed the highest uptake (standardized uptake value, SUV) in the occipital cortex (2.0), followed by the cerebellum (1.6), thalamus (1.5), and hippocampus (1.4). The lowest uptake of radioactivity was seen in the pons (0.4) (Figures 6A and 7A). As shown in the PET images (Figure 6B,C) and TACs (Figures 7B,C), pretreatment with MFTC or URB597 reduced the brain radioactivity. The radioactivity levels decreased rapidly within the first 5 min, then were followed by a slow washout in the brain. After MFTC administration, the radioactivity level in the occipital cortex and cerebellum at 90 min was reduced to about 80% and 74% of the control at 90 min, while that in the thalamus, hippocampus, and striatum decreased to 65–72% of the control. In the study with URB597, the ratios decreased about 50% at 90 min in the main brain regions and the highest ratio was 60% in the occipital cortex. Consistent with rats, the radioactivity levels in all brain regions were decreased by pretreatment with MFTC or URB597, suggesting that [^{11}C]MFTC has specific binding for FAAH in the monkey brain. It was found that URB597 (Figure 7C) blocked less of the radioactive signal in the control scan (Figure 7A) compared to MFTC (Figure 7B), suggesting that a small part of specific binding for [^{11}C]MFTC in the monkey brain is likely to be related to enzyme proteins other than FAAH.

To date, the distribution pattern of FAAH in the monkey brain and PET image of monkey brain with [^{11}C]CURB has not been reported. An immunohistochemical study indicated that FAAH protein was localized in the cerebral cortex, cerebellum, basal ganglia, and thalamus in the post-mortem

dx.doi.org/10.1021/cn500269g | ACS Chem. Neurosci. 2015, 6, 339–346

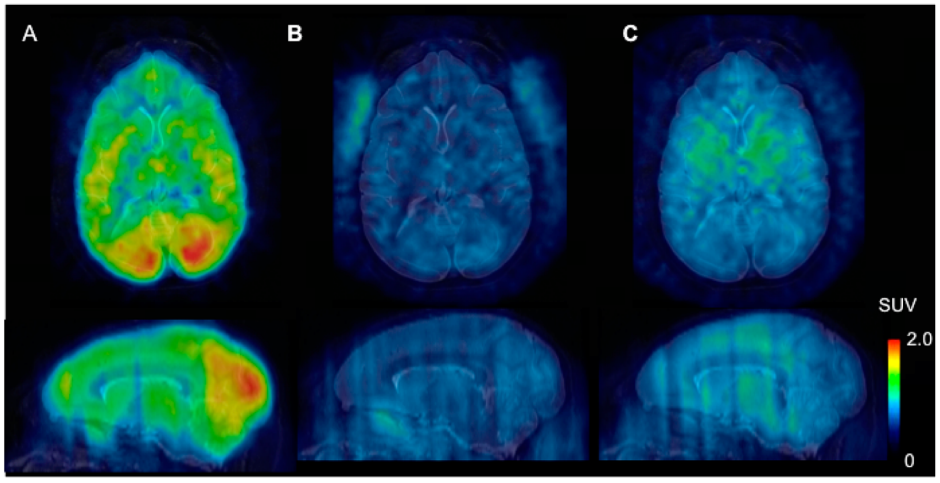

Figure 6. Representative PET/MR transverse (upper panels) and sagittal (lower panels) images for [^{11}C]MFTC in monkey brains. (A) [^{11}C]MFTC only. (B) Pretreatment with MFTC. (C) Pretreatment with URB597.

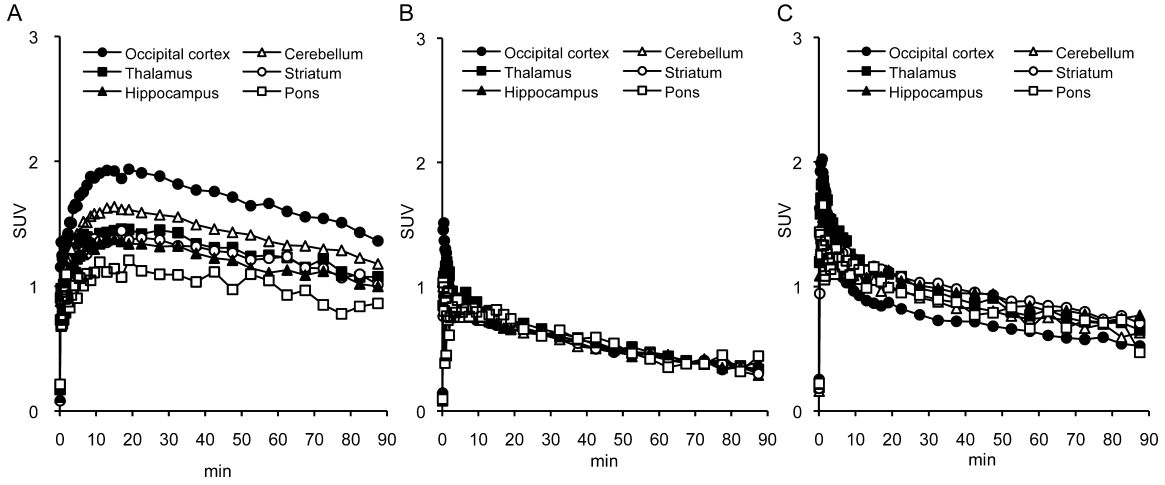

Figure 7. Time–activity curves for [^{11}C]MFTC in monkey brain. (A) [^{11}C]MFTC only. (B) Pretreatment with MFTC. (C) Pretreatment with URB597.

human brain.[4] Further, PET with [^{11}C]CURB also showed similar regional distribution of uptake in the human brain.[7] In this study on monkey, [^{11}C]MFTC displayed the highest specific binding in the occipital cortex and moderate or low specific binding throughout the brain regions. These results were similar to [^{11}C]CURB in the human brain and consistent with the wide distribution of FAAH in the human brain. However, compared to the high specific binding of [^{11}C]CURB in the striatum, [^{11}C]MFTC showed low binding in this region. [^{11}C]MK-3168, a reversible FAAH radiotracer, also had significant binding in the striatum.[15] The reason for this difference between [^{11}C]MFTC and [^{11}C]CURB or [^{11}C]MK-3168 remains unclear. A comparison of these radiotracers under the same experimental conditions may be required.

As an irreversible inhibitor for FAAH, PET with [^{11}C]MFTC for the rat brain showed that the uptake of radioactivity reached the maximum value at 30 min after the radiotracer injection and retained plateau from 30 min to the end (90 min) of PET scan. However, PET for the monkey brain showed that the uptake gradually decreased in the all regions examined after the radiotracer injection. No plateau of radioactivity in the brain regions was seen during the 90 min scan period. This result suggests the total binding determined in the TAC of monkey brain might be included by nonspecific binding to some extent. Thus, it may be difficult to quantify the specific binding of [^{11}C]MFTC for FAAH in the monkey brain from the TAC between 0 and 90 min. This is a limitation of [^{11}C]MFTC as a PET radiotracer for imaging and quantitative measurement of FAAH in primate brain. Considering the presence of nonspecific binding in the monkey brain, we will optimize the chemical structure of MFTC by decreasing lipophilicity (clogD value: 3.6) while maintaining potent binding affinity for FAAH, thus obtaining more suitable PET tracers for imaging and quantitative measurement of FAAH in primate brain.

In conclusion, in the present study, we have successfully synthesized and evaluated [^{11}C]MFTC as a novel radiotracer for PET imaging of FAAH in brain. [^{11}C]MFTC was synthesized using [^{11}C]$COCl_2$ via [^{11}C]carbonate, a new radioactive intermediate, in a short synthesis time and reliable radiochemical yield. PET studies of rat and monkey brains with [^{11}C]MFTC showed relatively high uptakes and specific binding with FAAH in the brains. [^{11}C]MFTC represents a promising radiotracer for visualizing FAAH in the brain. Optimization of this radiotracer is in progress.

dx.doi.org/10.1021/cn500269g | ACS Chem. Neurosci. 2015, 6, 339–346

METHODS

Materials and Methods. All chemicals and solvents were of analytic or high performance liquid chromatography (HPLC) grade from Aldrich (Milwaukee, WI) and Wako Pure Industries (Osaka, Japan). MFTC and two precursors, 3-hydroxy-2-methylpyridine (**2**) and 4-(5-(2-fluorophenyl)-4*H*-1,2,4-triazol-3-yl)piperidine (**3**), were synthesized in house (Supporting Information). Carbon-11 was produced by $^{14}N(p, \alpha)^{11}C$ nuclear reaction using a CYPRIS HM18 cyclotron (Sumitomo Heavy Industry, Tokyo, Japan). A dose calibrator (IGC-3R Curiemeter, Aloka, Tokyo) was used to measure all radioactivity if not otherwise stated. Reverse phase HPLC was performed using a JASCO system (JASCO, Tokyo). Effluent radioactivity was determined using a NaI (Tl) scintillation detector system.

Radiosynthesis of [^{11}C]MFTC. After irradiation, $[^{11}C]CO_2$ was recovered from the cyclotron target with N_2 and transferred into a heated methanizer full with nickel catalysts at 400 °C to produce $[^{11}C]CH_4$, which was then mixed with chlorine gas at 560 °C to give $[^{11}C]CCl_4$. Passage of $[^{11}C]CCl_4$ into a commercial glass tube containing iodine oxide and sulfuric acid at room temperature yielded $[^{11}C]COCl_2$.[18] The produced $[^{11}C]COCl_2$ was trapped in a solution of **2** (1 mg) in THF (300 μL) at −15 °C and this radioactive mixture was heated at 80 °C for 1 min. After the removal of THF a solution of **3**·HCl (1 mg) and diisopropylethylamine (7 μL) in DMF was added. The reaction mixture was then heated at 120 °C for 5 min.

Purification of this reaction mixture was conducted by semi-preparative HPLC on a Capcell Pack UG80 C_{18} column (10 mm internal diameter ×250 mm, Shiseido) using MeCN/H_2O (6/4) at 5.0 mL/min. The radioactive fraction corresponding to [^{11}C]MFTC (retention time: 8.5 min) was collected in a sterile flask, evaporated to dryness in vacuo, redissolved in 5 mL of sterile normal saline, and passed through a 0.22 μm Millipore filter to obtain [^{11}C]MFTC. The identity was confirmed by coinjecting the product with authentic MFTC on an analytic HPLC system (Capcell Pack UG80 C_{18} column, 4.6 mm × 250 mm) using MeCN/H_2O (6/4) at 1.0 mL/min (7.5 min). The specific activity was calculated by comparing the assayed radioactivity to the mass measured at UV 254 nm.

Animal Experiments. All animal experiments were performed according to the recommendations of the Committee for the Care and Use of Laboratory Animals, National Institute of Radiological Sciences. Animals were maintained and handled in accordance with the recommendations of the National Institute of Health and institutional guidelines of the National Institute of Radiological Sciences.

In Vitro Binding Affinity. The binding affinity (IC_{50}) for FAAH was examined using competitive activity-based protein profiling.[8] Membrane fractions of rat brain (50 μL, 1 mg/mL total protein concentration) were preincubated with varying concentrations of inhibitors at 37 °C. After 30 min, a fluorophosphonate-rhodamine probe (1 μL, 50 μM in DMSO) was added and the mixture was incubated for another 30 min at 37 °C. Reactions were quenched with SDS loading buffer, run on an SDS-PAGE gel, and visualized with a Fluor image analyzer FLA-5100 (GE Healthcare, Buckinghamshire, U.K.). Fluorescence of the relevant band at each inhibitor (MFTC and URB597) concentration was measured. Concentration−response curves were fit with GraphPad Prism 5 software (GraphPad Software, La Jolla, CA) to calculate the IC_{50} values.

Biodistribution Study in Mice. A saline solution of [^{11}C]MFTC (2 MBq, 0.05 pmol/200 μL) was injected into ddY mice (7 weeks, male) through the tail vein. Four mice were sacrificed by cervical dislocation at 1, 5, 15, 30, and 60 min after injection. Whole brain, heart, lung, liver, spleen, kidneys, small intestine, muscle, testes, and blood samples were quickly removed and weighed. The radioactivity present in these tissues was measured using a 1480 Wizard gamma counter (PerkinElmer Japan, Yokohama, Japan), and expressed as a percentage of the injected dose per gram of wet tissue (% ID/g). All radioactivity measurements were corrected for decay.

Small-Animal PET Study in Rat Brains. PET scans were conducted using a small-animal Inveon PET scanner (Siemens Medical Solutions, Knoxville, TN, USA), which provides 159 transaxial slices 0.796 mm apart (center-to-center), a 10 cm transaxial field of view (FOV), and a 12.7 cm axial FOV. Prior to the scans, rats were anesthetized with 5% (v/v) isoflurane and maintained thereafter with 1−2% (v/v) isoflurane. Emission scans were performed for 90 min after the intravenous injection of [^{11}C]MFTC (17 ± 3 MBq, 0.25−0.34 nmol). For the pretreatment studies, unlabeled MFTC or the FAAH-selective inhibitor URB597 (3 mg/kg) was dissolved in saline containing 10% ethanol and 5% Tween 80 and injected 30 min before the injection of [^{11}C]MFTC (17 ± 2 MBq, 0.20−0.30 nmol).

All list-mode acquisition data were sorted into three-dimensional sinograms, which were then Fourier rebinned into two-dimensional sinograms (frames × min: 4 × 1, 8 × 2, 14 × 5). Dynamic images were reconstructed with filtered back-projections using a Ramp's filter and a Nyquist cutoff of 0.5 cycle/pixel. Regions of interest (ROIs) were placed on the frontal cortex, striatum, thalamus, hippocampus, cerebellum, and pons using ASIPro VM (Siemens Medical Solutions USA) with reference to a template magnet resonance (MR) image of a rat brain. PET images were obtained by summing the uptake between 0−90 min after the injection of [^{11}C]MFTC. Each PET image was overlaid on the MR image, and a time−activity curve (TAC) for each brain region was acquired.

Brain radioactivity uptake was decay-corrected to the injection time and expressed as the standardized uptake value (SUV), normalized for injected radioactivity and body weight. SUV = (radioactivity per cubic centimeter tissue/injected radioactivity) × grams of body weight.

Determination of Irreversible Binding in Rat Brains. This experiment was performed according to the protocol reported previously.[6] Briefly, after intravenous injection of [^{11}C]MFTC (37 MBq, 0.5−0.9 nmol/200 μL) into rats, the rats were sacrificed at 1, 3, and 5 min (n = 3 for each point). Whole brain samples were removed quickly. For the inhibition study, URB597 (3 mg/kg) was injected 30 min before the injection of [^{11}C]MFTC (37 MBq, 0.82 nmol). The URB597-treated rats (n = 3) were sacrificed 5 min after the radiotracer injection. All of the brains were homogenized in 2.5 mL of ice-cold 80% MeCN/20% water and centrifuged (15 000*g*, 10 min, 4 °C). The supernatants were carefully decanted, and the pellets were resuspended in the same volume of extraction solvent. The procedure was repeated twice. The pellet and all supernatants from each rat were counted for radioactivity.

PET Study in Monkey. The PET scan was performed using an SHR-7700 PET scanner (Hamamatsu Photonics, Hamamatsu, Japan). This provides 31 transaxial slices 3.6 mm apart (center-to-center) and a 33.1 cm FOV. An MR image of the brain was obtained using a Philips Gyroscan S15/ACS II (1.5T) with a three-dimensional (3D) T1-weighted axial MR image sequence. A male rhesus monkey (*Macaca mulatta*) weighing approximately 6.0 kg was scanned while awake. A transmission scan for attenuation correction was subsequently performed for 20 min using a 74 MBq $^{68}Ge/^{68}Ga$ source. A dynamic scan in the 3D acquisition mode was conducted for 90 min (frames × min: 4 × 1, 8 × 2, 8 × 5, 3 × 10). A solution of [^{11}C]MFTC (110 MBq, 2 nmol) was injected into the monkey, and time-sequential tomographic scanning was performed for 90 min on transverse and sagittal sections of the brain. For the pretreatment studies, MFTC (1 mg/kg) or URB597 (3 mg/kg) was injected 30 min before the injection of [^{11}C]MFTC (110 MBq/2.4 nmol or 115 MBq/1.8 nmol). Emission scan images were reconstructed with a 4 mm Colsher filter, and circular ROIs with a 5 mm diameter were placed over the occipital cortex, cerebellum, striatum, hippocampus, thalamus, and pons using image analysis software. Each PET image was overlaid on the MR image of the monkey brain, and TAC for each brain region was determined. Brain uptake of radioactivity was decay-corrected to the injection time and expressed as SUV.

ASSOCIATED CONTENT

Supporting Information

Chemical synthesis of **1** and MFTC; Gel images for in vitro inhibition of FAAH by MFTC and URB597 as measured by competitive activity-based protein profiling; Ex vivo auto-

radiography of rat brain with [^{11}C]MFTC. This material is available free of charge via the Internet at http://pubs.acs.org.

AUTHOR INFORMATION

Corresponding Author

*Telephone: +81-43-382-3709. Fax: +81-43-206-3261. E-mail: zhang@nirs.go.jp.

Author Contributions

K. Kumata, M. O., Y. S., M. F., and K. Kawamura: chemical synthesis and radiosynthesis. J. Y., A. H., L. X., T. Y.: in vitro, mouse and rat experiments. J. M. and Y. N.: monkey experiment. K. Kumata, A. H., and M.-R. Z wrote the manuscript. M.-R. Z. conceived the experiments.

Notes

The authors declare no competing financial interest.

ACKNOWLEDGMENTS

We would like to thank the staff at the National Institute of Radiological Sciences for their support with the cyclotron operation, radioisotope production, radiosynthesis, and animal experiments.

ABBREVIATIONS

FAAH, fatty acid amide hydrolase; % ID/g, percentage of the injected dose per gram of wet tissue; MR, magnet resonance; PET, positron emission tomography; SUV, standardized uptake value; TAC, time−activity curve

REFERENCES

(1) Cravatt, B. F., Giang, B. K., Mayfield, S. P., Boger, D. L., Lerner, R. A., and Gilula, N. B. (1996) Molecular characterization of an enzyme that degradesneuromodulatory fatty-acid amides. *Nature 384*, 83−87.

(2) Piomelli, D. (2003) The molecular logic of endocannabinoid signaling. *Nat. Rev. Neurosci. 4*, 873−884.

(3) Ahn, K., McKinney, M. K., and Cravatt, B. F. (2008) Enzymatic pathways that regulate endocannabinoid signaling in the nervous system. *Chem. Rev. 108*, 1687−1707.

(4) Romero, J., Hillard, C. J., Calero, M., and Rábano, A. (2002) Fatty acid amide hydrolase localization in the human central nervous system: An immunohistochemical study. *Mol. Brain Res. 100*, 85−93.

(5) Pacher, P., and Kunos, G. (2013) Modulating the endocannabinoid system in human health and disease − successes and failures. *FEBS J. 280*, 1918−1943.

(6) Wilson, A. A., Garcia, A., Parkes, J., Houle, S., Tong, J., and Vasdev, N. (2011) [^{11}C]CURB: Evaluation of a novel radiotracer for imaging fatty acid amide hydrolase by positron emission tomography. *Nucl. Med. Biol. 38*, 247−253.

(7) Rusjan, P. M., Wilson, A. A., Mizrahi, R., Boileau, I., Chavez, S. E., Lobaugh, N. J., Kish, S. J., Houle, S., and Tong, J. (2013) Mapping human brain fatty acid amide hydrolase activity with PET. *J. Cereb. Blood Flow Metab. 33*, 407−414.

(8) Skaddan, M. B., Zhang, L., Johnson, D. S., Zhu, A., Zasadny, K. R., Coelho, R. V., Kuszpit, K., Currier, G., Fan, K. H., Beck, E. M., Chen, L., Drozda, S. E., Balan, G., Niphakis, M., Cravatt, B. F., Ahn, K., Bocan, T., and Villalobos, A. (2013) The synthesis and in vivo evaluation of [^{18}F]PF-9811: A novel PET ligand for imaging brain fatty acid amide hydrolase (FAAH). *Nucl. Med. Biol. 40*, 1058−1067.

(9) Wilson, A. A., Hicks, J. W., Sadovski, O., Parkes, J., Tong, J., Houle, S., Fowler, C. J., and Vasdev, N. (2013) Radiosynthesis and evaluation of [^{11}C-carbonyl]-labeled carbamates as fatty acid hydrolase radiotracers for positron emission tomography. *J. Med. Chem. 56*, 201−208.

(10) Hicks, J. W., Parkes, J., Sadovski, O., Tong, J., Houle, S., Vasdev, N., and Wilson, A. A. (2013) Synthesis and preclinical evaluation of [^{11}C-carbonyl]PF-04457845 for neuroimaging of fatty acid amide hydrolase. *Nucl. Med. Biol. 40*, 740−746.

(11) Sadovski, O., Hicks, J. W., Parkes, J., Raymond, R., Nobrega, J., Houle, S., Cipriano, M., Fowler, C. J., Vasdev, N., and Wilson, A. A. (2013) Development and characterization of a promising fluorine-18 labelled radiopharmaceutical for in vivo imaging of fatty acid amide hydrolase. *Bioorg. Med. Chem. 21*, 4351−4357.

(12) Rotstein, B. H., Wey, H. Y., Shoup, T. M., Wilson, A. A., Liang, S. H., Hooker, J. M., and Vasdev, N. (2014) PET imaging of fatty acid amide hydrolase with [^{18}F]DOPP in nonhuman primates. *Mol. Pharmaceutics 11*, 3832−3838.

(13) Pandey, M. K., DeGrado, T. R., Qian, K., Jacobson, M. S., Hagen, C. E., Duclos, R. I., Jr., and Gatley, S. J. (2014) Synthesis and preliminary evaluation of N-(16-^{18}F-Fluorohexadecanoyl)-ethanolamine (^{18}F-FHEA) as a PET probe of N-acylethanolamine metabolism in mouse brain. *ACS Chem. Neurosci. 5*, 793−802.

(14) Li, W., Sanabria-Bohorquez, S., Joshi, A., Cook, J., Holahan, M., Posavec, D., Purcell, M., DeVita, R., Chobanian, H., Liu, P., Chioda, M., Nargund, R., Lin, L., Zeng, Z., Miller, P., Chen, T., O'Malley, S., Riffel, K., Williams, M., Bormans, G., Van Laere, K., De Groot, T., Evens, N., Serdons, K., Depre, M., de Hoon, J., Sullivan, K., Hajdu, R., Shiao, L. L., Alexander, J., Blanchard, R., DeLepeleire, I., Declercq, R., Hargreaves, R., and Hamill, T. (2011) The discovery and characterization of [^{11}C]MK-3168, a novel PET tracer for imaging fatty acid amide hydride (FAAH). *J. Labelled Compd. Radiopharm. 54*, S38.

(15) Liu, P., Hamill, T. G., Chioda, M., Chobanian, H., Fung, S., Guo, Y., Chang, L., Bakshi, R., Hong, Q., Dellureficio, J., Lin, L. S., Abbadie, C., Alexander, J., Jin, H., Mandala, S., Shiao, L. L., Li, W., Sanabria, S., Williams, D., Zeng, Z., Hajdu, R., Jochnowitz, N., Rosenbach, M., Karanam, B., Madeira, M., Salituro, G., Powell, J., Xu, L., Terebetski, J. L., Leone, J. F., Miller, P., Cook, J., Holahan, M., Joshi, A., O'Malley, S., Purcell, M., Posavec, D., Chen, T. B., Riffel, K., Williams, M., Hargreaves, R., Sullivan, K. A., Nargund, R. P., and DeVita, R. J. (2013) Discovery of MK-3168: A PET tracer for imaging brain fatty acid amide hydrolase. *ACS Med. Chem. Lett. 4*, 509−513.

(16) Aoki, A., Munagata, R., Kawano, N., Samizu, K., Oka, H., Ishii, T., and Sugane, T. (2010) Azole Compound. Patent WO2010/007966A1.

(17) Pike, V. W. (2009) PET radiotracers: Crossing the blood-brain barrier and surviving metabolism. *Trends Pharmacol. Sci. 30*, 431−440.

(18) Ogawa, M., Takada, Y., Suzuki, H., Nemoto, K., and Fukumura, T. (2010) Simple and effective method for producing [^{11}C]phosgene using an environmental CCl_4 gas detection tube. *Nucl. Med. Biol. 37*, 73−76.

(19) Takada, Y., Ogawa, M., Suzuki, H., and Fukumura, T. (2010) Radiosynthesis of [2-^{11}C-carbonyl]dantrolene using [^{11}C]phosgene for PET. *Appl. Radiat. Isot. 68*, 1715−1720.

(20) Wilson, A. A., Garcia, A., Houle, S., and Vasdev, N. (2010) Direct fixation of [^{11}C]-CO2 by amines: Function of [11C-carbonyl]-methylcarbamates. *Org. Biomol. Chem. 8*, 428−432.

(21) Kawamura, K., Hashimoto, H., Ogawa, M., Yui, J., Wakizaka, H., Yamasaki, T., Hatori, A., Xie, L., Kumata, K., Fujinaga, M., and Zhang, M. R. (2013) Synthesis, metabolite analysis, and in vivo evaluation of [(11)C]irinotecan as a novel positron emission tomography (PET) probe. *Nucl. Med. Biol. 40*, 651−657.

(22) Fowler, C., Jonsson, K. O., and Tiger, G. (2001) Fatty acid amide hydrolase: Biochemistry, pharmacology, and therapeutic possibilities for an enzyme hydrolyzing anandamide, 2-arachidonoylglycerol, palmitoylethanolamide, and oleamide. *Biochem. Pharmacol. 62*, 517−526.

(23) Watanabe, K., Ogi, H., Nakamura, S., Kayano, Y., Matsunaga, T., Yoshimura, H., and Yamamoto, I. (1998) Distribution and characterization of anandamide amidohydrolase in mouse brain and liver. *Life Sci. 62*, 1223−1229.

(24) Hillard, C. J., Wilkison, D. M., Edgemond, W. S., and Campbell, W. B. (1995) Characterization of the kinetics and distribution of *N*-arachidonylethanolamine (anandamide) hydrolysis by rat brain. *Biochem. Biophys. Acta. 1257*, 249−256.

(25) Thomas, E. A., Cravatt, B. F., Danielson, P. E., Gilula, N. B., and Sutcliffe, J. G. (1997) Fatty acid amide hydrolase, the degradative enzyme for anadamide and oleamide, has selective distribution in neurons within the rat central nervous system. *J. Neurosci. Res. 50*, 1047−1052.